Atti e Memorie della Commissione Grotte "E. Boegan"	Volume n.51	pp. 41 - 59	Trieste 2021- 2022

Andrea Bussani[1]

SEASONAL CHARACTERISTICS OF ATMOSPHERIC THERMAL TIDES IN "COSTANTINO DORIA" CAVE (N. 3875 V.G.)

RIASSUNTO

Dal 25 aprile 2019 all'8 maggio 2021 all'interno della grotta "Costantino Doria", situata sul carso triestino, sono state raccolte mediante uno strumento digitale programmabile serie temporali di temperatura dell'aria e di pressione atmosferica. L'analisi dei dati ha evidenziato la presenza di due stagioni principali all'interno della cavità: una stagione fredda (approssimativamente da metà novembre a metà aprile), caratterizzata da intensi scambi termici e d'aria con l'ambiente esterno, e una stagione calda (approssimativamente da metà aprile a metà novembre), in cui tali scambi sono alquanto ridotti. Durante la stagione fredda, la temperatura dell'aria della grotta Doria è dominata dal consueto ciclo diurno di riscaldamento/raffreddamento; nella stagione calda, invece, gli scambi termici e di massa molto ridotti con l'ambiente esterno consentono di osservare in modo estremamente chiaro le oscillazioni del segnale di temperatura dovute alla compressione/espansione dell'atmosfera della grotta, causate a loro volta dalle maree atmosferiche termiche nonché dagli scambi termici con le pareti della cavità. Relativamente alla stagione calda, viene anche analizzato il ritardo di fase tra il segnale della temperatura dell'aria e quello della pressione atmosferica della grotta, confrontandolo con gli altri valori disponibili in letteratura.

ABSTRACT

From 25/04/2019 to 08/05/2021, in "Costantino Doria" cave, a karstic cavity near Trieste (Italy), the time series of atmospheric pressure and air temperature were collected by means of a self-recording programmable logger. The data analysis showed that two main seasons occur in Doria cave: a cold season (approximately from mid-November to mid-April), characterised by intense heat and air exchanges with the outside environment,

[1]Andrea Bussani, Via Leopoldo Mauroner, 14, Trieste, 34142, Italy
andrea.bussani@gmail.com

and a hot season (approximately from mid-April to mid-November), when such exchanges are remarkably fewer. During the cold season, the air temperature of Doria cave is dominated by the usual heating/cooling processes that takes place during the day; on the contrary, during the hot season, the sharp reduction of both heat and air exchanges allows to observe very clearly the air temperature oscillations caused by the compression/ expansion of the atmosphere of the cave, induced by the atmospheric thermal tides as well as by the heat exchanges between the cave air mass and the rock walls. The phase-lag, observed between the air temperature and the atmospheric pressure signals during the hot season, is also analysed and compared to the results of previous works available in literature.

INTRODUCTION

Starting from 1957, the meteorological characteristics of "Costantino Doria" cave[1] (N. 3875 V.G.; hereafter Doria cave; Fig. 1), a karstic cavity near Trieste (Italy), have been investigated by several researchers (see, for example: Forti & Tommasini, 1957; Polli, 1969; Choppy, 1980).

In summer 2001, a new research campaign was undertaken, aiming to investigate the air temperature of Doria cave at a much higher sampling rate (10 minutes) than previous works, using a self-recording programmable thermometer (Bussani, 2005). Surprisingly enough, a well-defined semidiurnal constituent was detected in the air temperature signal. The authors surmised that it was an effect of the atmospheric thermal tides because these are characterised by a marked semidiurnal pattern as well. However, such hypothesis was questioned by the authors themselves since the cause-effect mechanism was then unclear. Most puzzlingly, a phase-lag was present between the semidiurnal constituent of the external atmospheric pressure and that of the underground air temperature, with the latter unexpectedly peaking about three hours before the semidiurnal constituent of external pressure. Similar results were found in "Abisso di Trebiciano" cave in 2006 (Bussani, 2007), though in this case the observed phase-lag was less than two hours long.

Bibliographical research showed that this phenomenon had already been detected in 2000 by Chen et al. (2003) in an artificial cavity, i.e., an underground scientific laboratory. A model of heat conduction between air and rock had then been devised by Wu et al. (2003) to explain the phase-lag. As a matter of fact, the model was in rather close agreement with the measurements collected in the underground laboratory.

Such important experimental and theoretical results notwithstanding, we deemed it beneficial to acquire new experimental data and further investigate the physical processes that govern these phenomena, in order to better understand the temporal variations of the semidiurnal oscillations of the air temperature in caves. Actually, we were not able to find

[1] For a detailed account (in Italian) of the history of the research activities in "Costantino Doria" cave, see https://www.catastogrotte.it/grotta/724 and references therein.

any papers about this topic; moreover, the differences in the phase-lag estimations observed by Bussani (2005, 2007) and Chen et al. (2003) and Wu et al. (2003) are rather conspicuous. Consequently, in April 2019 we started a new series of measurements of both the atmospheric pressure and the air temperature of Doria cave, to have a larger dataset available for the temporal characterisation of these two parameters. The research activity ended in May 2021.

Doria cave was chosen because of the many scientific studies previously conducted in this cave. In addition to that, the cave is easily accessible, and it is not open to the public, the entrance being closed by a grate. In fact, the choice of implementing our research activity in Doria cave could have come with a major downside, since both lower ends of Doria cave – the eastern and the western – communicate with other cavities (Fig. 2), i.e., with cave N. 3876 and cave N. 21, respectively. However, the passage between cave N. 3876 and Doria cave is extremely narrow and not even visible; the passage between Doria cave and cave N. 21 is slightly wider, though still inaccessible, and more importantly, the entrance of cave n. 21 is known to have been blocked long before 2019. Consequently, Doria cave was an ideal site to conduct a new study about atmospheric thermal tides.

In this paper we present the results of our research.

DATA COLLECTION AND DATA ANALYSIS METHODS

The data about air temperature and atmospheric pressure of Doria cave were collected by means of a Driesen und Kern Plog 520 programmable data logger (serial number: 521005522). The technical specifications of the instrument are given in Tab. 1 (taken from Bussani, 2007).

Length	200 mm
Diameter	23 mm
Memory	500000 measurements
Pressure accuracy	20 Pa
Pressure resolution	15 Pa
Temperature accuracy	0.1 °C
Temperature resolution	0.003 °C

Table 1: Technical specifications of the Driesen und Kern Plog 520 programmable data logger (from Bussani, 2007).

Occasionally, a second logger (serial number: 520604421) with the same technical characteristics was used to check for possible anomalies and malfunctions of the main logger. The recordings started on 25/04/2019 and ended on 08/05/2021. The time interval between two consecutive measurements (i.e., sampling time) was either 10 seconds or 20 seconds (see Tab. 2).

Data segment	Air temperature	Atmospheric pressure	Sampling interval (s)
1	s: 26/04/2019 00:00 e: 15/06/2019 19:06	s: 25/04/2019 18:01 e: 15/06/2019 19:06	Δt=10
2	s: 19/06/2019 00:00 e: 12/08/2019 15:18	s: 16/06/2019 18:01 e: 12/08/2019 15:18	Δt=10
3	s: 17/08/2019 00:00 e: 11/10/2019 17:18	s: 16/08/2019 02:01 e: 11/10/2019 17:18	Δt=10
4	s: 14/10/2019 00:00 e: 24/11/2019 04:37	s: 13/10/2019 21:01 e: 24/11/2019 04:38	Δt=10
5	s: 16/12/2019 00:01 e: 20/03/2020 09:45	s: 16/12/2019 00:01 e: 20/03/2020 09:45	Δt=10
6	s: 17/05/2020 18:01 e: 17/07/2020 11:38	s: 17/05/2020 18:01 e: 17/07/2020 11:38	Δt=20
7	s: 19/07/2020 00:00 e: 30/09/2020 16:40	s: 19/07/2020 00:00 e: 30/09/2020 16:40	Δt=20
8	s: 09/10/2020 03:00 e: 13/01/2021 13:37	s: 08/10/2020 22:01 e: 13/01/2021 13:37	Δt=20
9*	s: 15/01/2021 00:01 e: 08/05/2021 18:06	s: 15/01/2021 00:01 e: 08/05/2021 18:06	Δt=20

Table 2: Air temperature and atmospheric pressure data segments: "s" and "e" stand for measuring start time and end time, respectively; times are given in the dd/mm/yyyy hh:mm format; "sampling interval" is the time elapsed between two consecutive measurements in the raw data (i.e., before computing the minute-average); the asterisk in data segment 9 shows that those data were recorded by a different logger.

The latter was chosen further on in the research to save battery life and not risk any data loss caused by power shortage. The logger was periodically retrieved to download the data; after the download procedure, the logger was again deployed in the same place. The whole procedure usually took a couple of days up to slightly over a week. However, two longer periods without measurements occurred: from 24/11/2019 to 16/12/2019, the logger did not record any measurements, probably due to power issues; from 20/03/2020 to 17/05/2020 the logger could not be retrieved due to Covid restriction rules, because of which no one was allowed to leave their homes. After each retrieval, the data were visually checked for anomalous values: in fact, only air temperature measurements recorded soon after deployment (i.e., up to three days after deployment) and air temperature and atmospheric pressure measurements recorded during and after retrieval were removed. After data cleaning, for each parameter the minute-averages (i.e., the average computed over a time span of one minute) were worked out and used for the data analysis. For the sake of clarity, for each parameter, "data segment" defines the time series of the minute-

averages – computed after the removal of unusable data – of the measurements recorded between the instrument deployment and the subsequent retrieval; also, for each parameter, "time series" defines the whole set of all data segments in chronological order. According to these definitions, both the air temperature and the atmospheric pressure data series are made up of nine data segments (Tab. 2); more specifically, the air temperature and the atmospheric pressure data series consist of 925031 and 930426 minute-averaged values, respectively (a larger number of air temperature measurements with respect to atmospheric pressure measurements were removed since air temperature of the cave was noticeably more affected by the presence of the researchers, which caused perturbations of the atmosphere of the cave). The measurements of the data segment n. 9 were recorded using the S/N 520604421 Plog 520 logger. Since both instruments had been previously used in data segment 7 – S/N 521005522 as the main logger and S/N 520604421 as the control logger – the constant (i.e., not-drifting) biases of air temperature and atmospheric pressure between the two instruments were corrected and removed.

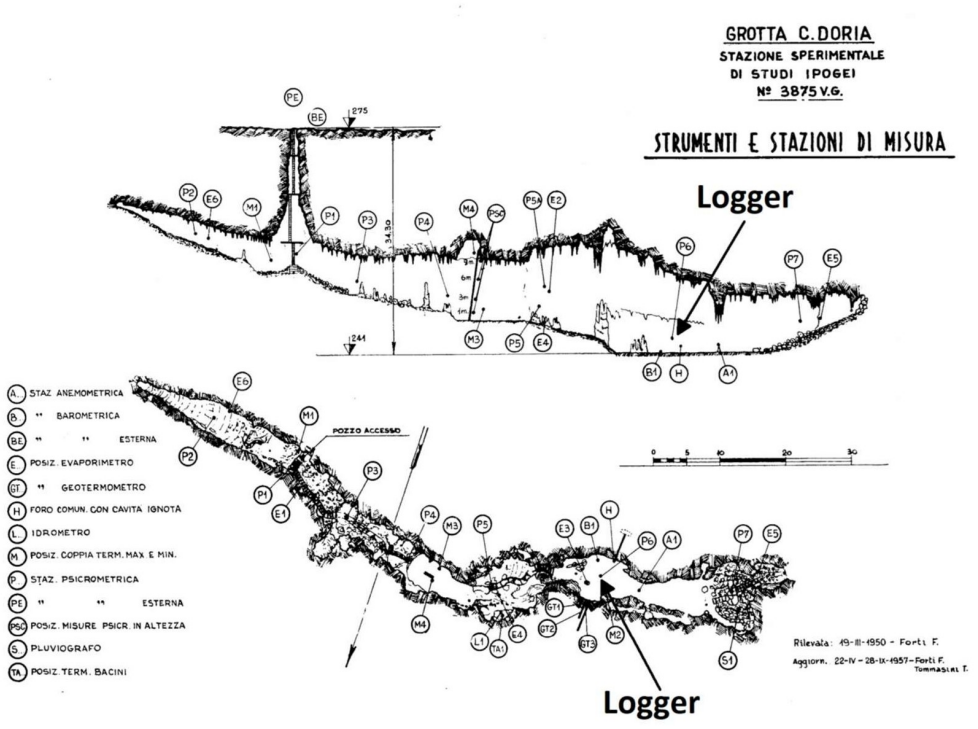

Figure 1: Logger position in the cave (adapted from Polli, 1969).

To perform the spectral analysis of the atmospheric pressure and the air temperature time series of Doria cave, for each parameter the 24-hours moving average was computed; then, the residuals (24-hours moving average subtracted from the corresponding minute-average) were worked out. Zero-padding was applied to the time series of the residuals when measurements were missing.

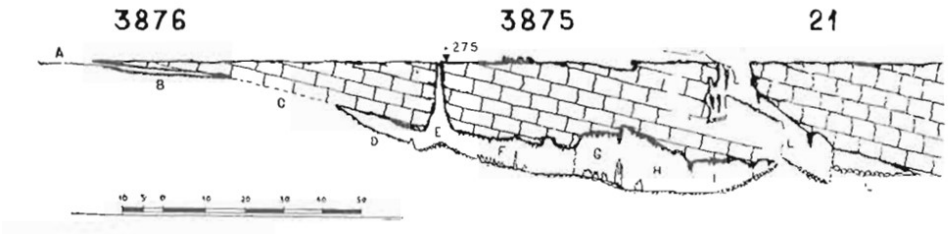

Figure 2: Position of caves N. 3876 and N. 21, communicating with Doria cave, N. 3875 (from Choppy (1980), taken in turn from Forti (1961)).

GNU Octave software (Eaton et Al., 2022) was used to calculate the Fast Fourier Transform of each time series, whereas R CRAN software was used for data manipulation, descriptive statistical analysis and plotting the figures. The air temperature data of Borgo Grotta Gigante weather station – used for subsequent statistical analyses – belong to the ARPA-OSMER Regional Meteorological Observatory of the Regional Agency for Environmental Protection of Friuli Venezia Giulia and were downloaded from the ARPA-OSMER website.

RESULTS AND DISCUSSION

1. Time-domain analysis of air temperature

Doria cave is less than one kilometre away from the hamlet of Borgo Grotta Gigante (BGG hereafter). The time series of both the air temperature recorded at BGG weather station from 2019 up to 2021 and that recorded in Costantino Doria cave (CD hereafter) are plotted in Fig. 3. It is clear that CD air temperature is characterized by an extreme stability, compared to BGG temperature. A first visual inspection of the plot would suggest that CD air temperature is about the average value of the external (BGG) temperature; however, a more accurate analysis was performed only on the measurements collected when the logger was recording, i.e., from 26/04/2019 up to 08/05/2021, and deleting BGG measurements taken when the logger was not deployed or not functioning. This proved that BGG air temperature fluctuated between a minimum value of -3.0 °C and a maximum value of 28.1 °C with an average value of 13.2 °C, whereas CD air temperature ranged between 10.78 °C and 11.72 °C with an average value of 11.33 °C. These statistics bring out two interesting points:

- A moderate increase in the measured air temperature of the cave with respect to historical values: actually, in the measuring point P6 (Fig. 1) that is next to the logger position, in 1963-1969 Polli (1969) never observed temperatures higher than 11.30 °C. Additionally, the CD air temperature as measured in this research ranges in a distinctly narrower interval than what observed by Polli (1969), who in 1963 measured air temperature as low as 7.30 °C. However, over the years, some excavations have allegedly been conducted in the cave that may have significantly affected the inner air circulation; above all, the aforementioned block of the entrance of cave N.21 may have largely contributed to the reduction of heat and air exchanges with the outside environment.

- The considerable difference between the CD and the BGG air temperatures, the cave being about 1.9 °C colder than outside. Polli (1969) had previously found that such difference was 1 °C, but, as already mentioned, such a minor discrepancy may be due to the changes in the morphology of the cave over the years.

Despite the extremely narrow range of CD air temperature compared to the external air temperature (Fig. 3), by zooming in the vertical axis and focusing on the daily variability of the CD air temperature, it is possible to identify a neat pattern in the cave temperature signal (Fig. 4) characterised by:

- A "hot season", approximately from mid-April to mid-November: during this period, the cave temperature slowly rises, and the daily temperature variations are extremely small, i.e., about some hundredths of degree.
- A "cold season" during the other months, characterised by an abrupt drop in the cave temperature in November, followed by a rise starting from January-February; more interestingly, during the cold season, the cave temperature variations are about one order of magnitude larger than those observed during the hot season, with daily oscillations that can be up to slightly more than one tenth of degree.

A possible explanation of this scenario is the following: in November, as soon as the external temperature reaches a value lower than that of the cave, the denser external air starts to sink into the cave, thus causing a dramatic change in the CD air temperature. Such downward vertical movements continue as long as the mean external temperature is persistently lower than that of the cave; Fig. 3 may help define this time span, essentially corresponding to the months during which BGG air temperature is lower than CD air temperature.

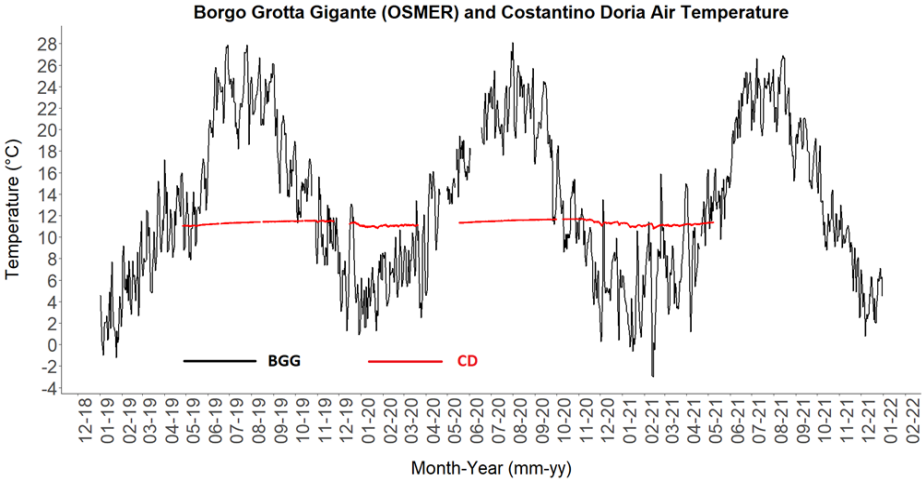

Figure 3: Air temperature time series recorded at Borgo Grotta Gigante weather station (BGG) and Doria cave (CD) air temperature (BGG data provided by OSMER-FVG weather observatory).

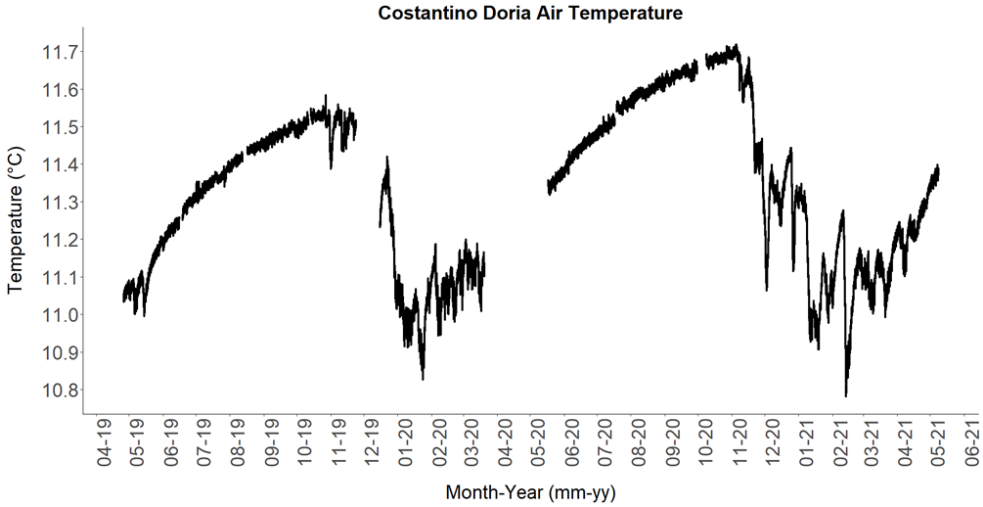

Figure. 4: Air temperature time series recorded at Doria cave.

As a matter of fact, most of the cooling process takes place in just three months, roughly from November to January; the coldest days are recorded in February, confirming the great variability of the cold season. However, once the external temperature rises higher than the temperature inside the cave, the downward air ingressions stop and the heating process inside the cave starts to proceed steadily, with the rock walls transferring heat to the cave atmosphere. During the hot season, the lack of cold air ingressions from outside prevents the cave temperature from changing as swiftly and sharply as during the cold season.

In fact, the annual cycle of the cave temperature was thoroughly discussed by Polli (1969) and Choppy (1980) (Fig.5) in their works. Nevertheless, thanks to the higher sampling frequency of the logger used in the 2019-2021 campaign, we were able to provide a quantitative description of the variability of the cave temperature about the daily mean over the year. As far as we know, this is the first time that this kind of analysis has been performed. Polli (1969) also suggested that Doria cave trapped cold air during winter and that it got slowly heated by the rock walls in spring, summer and early autumn; we con-

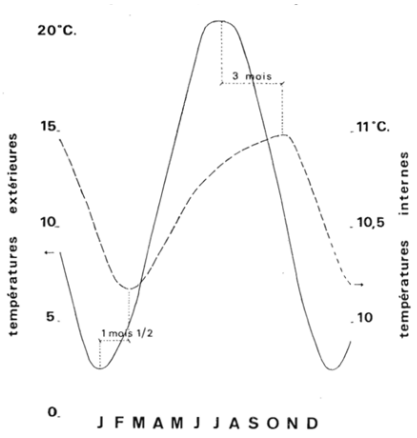

Figure 5: Mean annual cycle of the external ("températures exteriéures", solid line) and of the internal temperature ("températures internes", dashed line) of the "C. Doria" cave; on the x-axis the different months are reported; "mois" stands for "month" (from Choppy, 1980).

firm this hypothesis and provide a detailed picture of the abrupt and pronounced drops and spikes that occur in November-February, both in 2019 and 2020.

It is interesting to note that the air temperature pattern of the cave is similar to the well-known behaviour of an RC circuit, with the charge/discharge processes being replaced by the heating/cooling of the cave.

2. Frequency-domain analysis of atmospheric pressure and air temperature

On the grounds of the results of the time-domain analysis, data were grouped into two clusters, corresponding to the two seasons observed in Doria cave (Tab. 3), though the lack of data in some months led to a certain level of inaccuracy in the season definition. Successively, for each parameter, the residuals (i.e., 24-hours moving average subtracted from the minute-averages) were computed; finally, on the time series of the residuals, a spectral analysis was performed to look for the presence of periodical constituents. The results are given in Figs. 6-13.

Cave	Acronym	Start and end date
Spring-Summer 2019	SS1	s: 15/05/2019 e: 26/10/2019
Autumn-Winter	AW1	s: 27/10/2019 e: 19/03/2020
Spring-Summer 2020	SS2	s: 18/05/2020 e: 05/11/2020
Autumn-Winter	AW2	s: 06/11/2020 e: 18/04/2021

Table 3: Seasons definition for the spectral analysis of the air temperature and atmospheric pressure signals: "s" and "e" stand for measuring start time and end time; dates are expressed in the dd/mm/yyyy format.

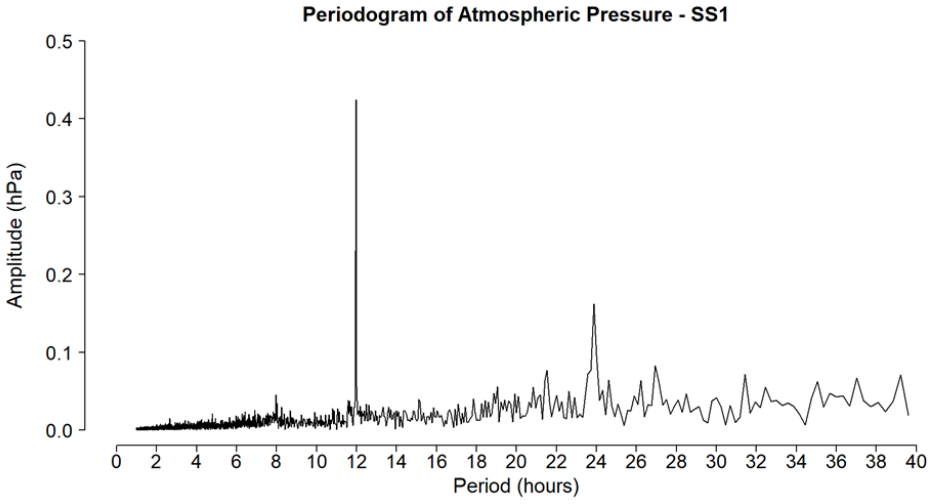

Figure 6: Periodogram (amplitude vs period) of atmospheric pressure in Doria cave during season SS1.

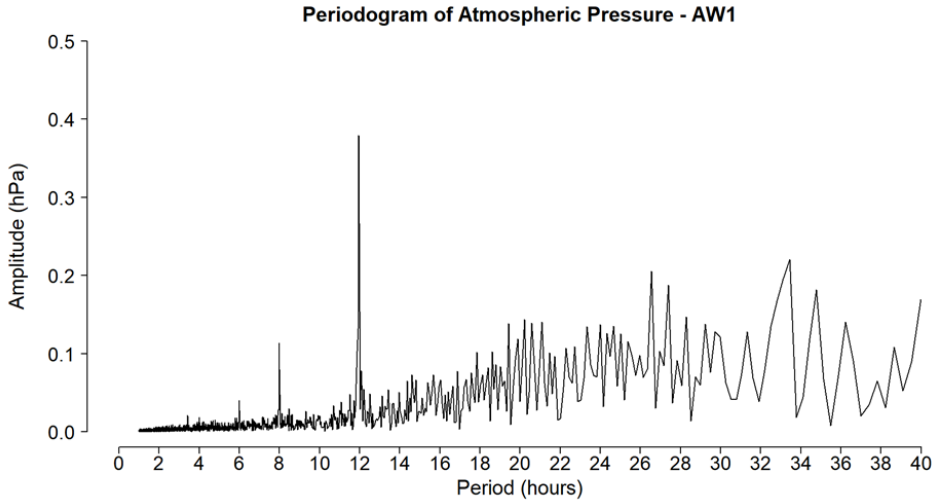

Figure 7: Periodogram (amplitude vs period) of atmospheric pressure in Doria cave during season AW1.

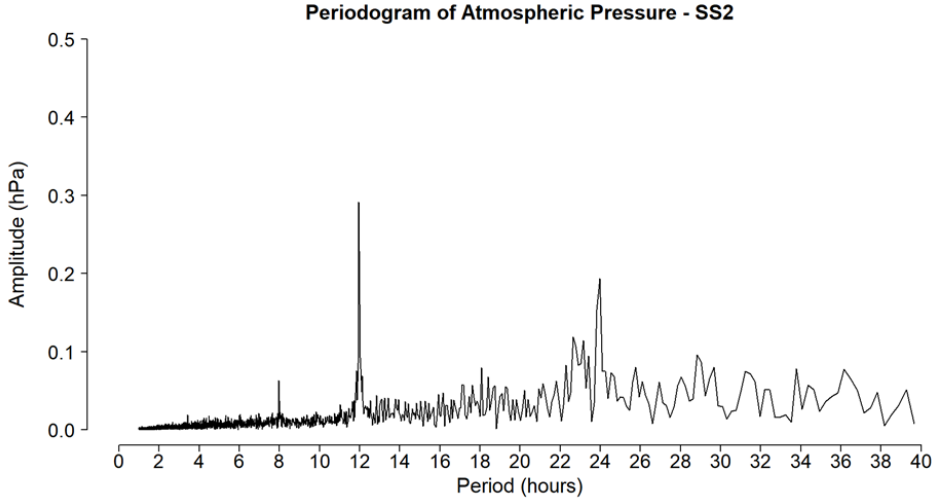

Figure 8: Periodogram (amplitude vs period) of atmospheric pressure in Doria cave during season SS2.

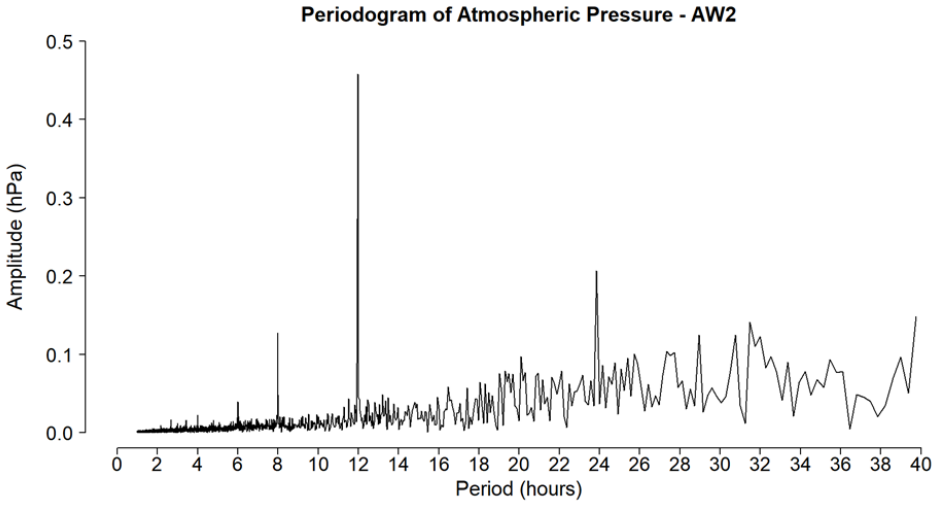

Figure 9: Periodogram (amplitude vs period) of atmospheric pressure in Doria cave during season AW2.

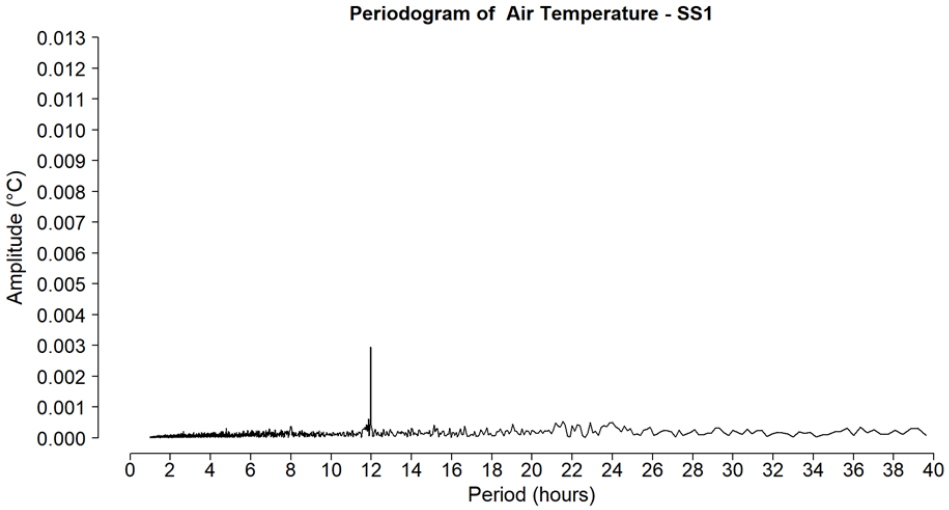

Figure 10: Periodogram (amplitude vs period) of air temperature in Doria cave during season SS1.

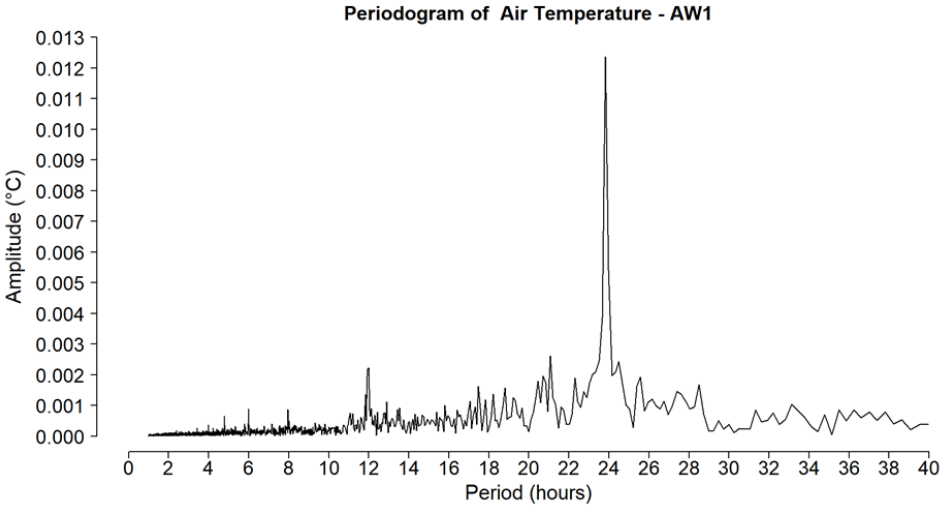

Figure 11: Periodogram (amplitude vs period) of air temperature in Doria cave during season AW1.

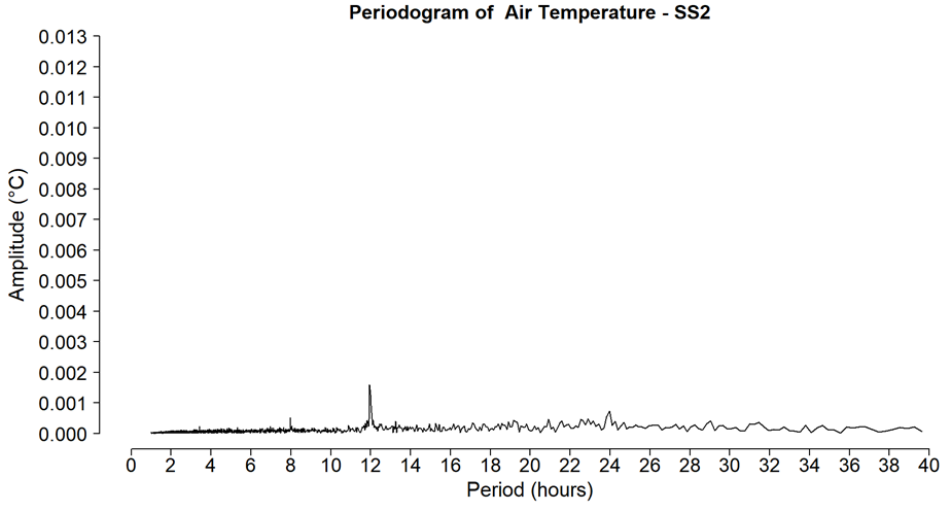

Figure 12: Periodogram (amplitude vs period) of air temperature in Doria cave during season SS2.

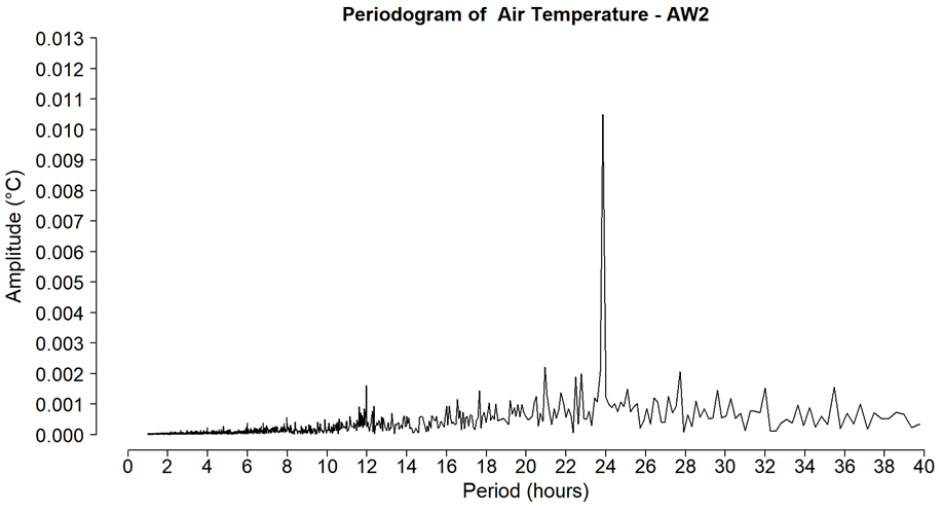

Figure 13: Periodogram (amplitude vs period) of air temperature in Doria cave during season AW2.

The periodograms (amplitude vs period) of the atmospheric pressure of the cave (Figs 6-9) essentially show the same pattern, regardless of the season. Actually, there is a main peak, corresponding to the semidiurnal (12 h) constituent, whose amplitude approximately ranges between 0.3 and 0.5 hPa; a second, lower peak, corresponding to the diurnal (24 h) constituent and whose amplitude is about 0.2 hPa, is clearly visible in all seasons but AW1, however in season AW1 the logger was not recording for a considerable number of winter months, making the AW1 periodogram the less reliable of all; furthermore, a number of minor peaks can be seen in the four periodograms, corresponding to the periods of higher harmonics.

Unlike the atmospheric pressure, in the periodograms of the air temperature (Figs. 10-13) the seasonal dependence of the pattern emerges in a striking way: while the semidiurnal constituent – having an amplitude of about 0.002-0.003 °C – is present in all four plots, the diurnal constituent is observed only in the two cold seasons, AW1 and AW2, but it is totally absent in the hot seasons, SS1 and SS2; also, in both AW1 and AW2 the amplitude of the diurnal constituent is one order of magnitude larger than the semidiurnal constituent.

3. Mean daily cycles of atmospheric pressure and air temperature

For each examined season, the mean daily cycles of the atmospheric pressure and of the air temperature of the cave were worked out by averaging all the minute-average values corresponding to the same time of day (i.e., same hour and same minute regardless of the date) (Figs. 14-15). These calculations were made on the time series of the residuals to avoid the influence of the trend. Matching what we found out in the frequency-domain analysis, the mean daily cycle of the atmospheric pressure of the cave (Fig. 14) is totally

independent from the season: two maxima and two minima are clearly visible in the plot, although in both hot seasons the first minimum occurs slightly earlier than in the cold seasons, whereas the second minimum is observed slightly later; this can be presumably due to the increased number of daylight hours during the hot seasons. However, the mean daily cycle of the air temperature of the cave clearly depends on the season (Fig. 15): in the hot seasons the semidiurnal pattern is very neat, with two maxima occurring approximately at 8 am and 9 pm, and two minima approximately at 3 am and 3 pm, with the maximum deviations from the mean being about 0.003 °C. On the contrary, in the cold seasons the diurnal pattern takes over, with the minimum occurring at about 7 am and the maximum at about 4 pm, and with much larger deviations from the mean, the maximum deviation being about 0.015 °C. As explained before, these two completely different scenarios are due to the completely distinct air circulation patterns which take place in Doria cave over the year: an extremely stable cave atmosphere in the hot season, when the thermal variations on a daily time scale are primarily induced by the atmospheric thermal tides, and external air ingressions into the cave – with the consequent heat exchange – in the cold seasons, causing the air temperature of the cave to fluctuate according to the external temperature.

4. Phase-lag between atmospheric pressure and air temperature

For each season, we drew on the same plot the mean daily cycles of the time series of the residuals of both the atmospheric pressure and the air temperature of the cave (Figs. 16-19). The now well-known seasonal dependence of the air temperature pattern is once again clear. However, from the plots of season SS1 and SS2 an extremely important result emerges, i.e. the presence of a phase-lag between the atmospheric pressure and the air temperature signals. More specifically, the air temperature signal is ahead of the air pressure signal of about slightly more than 1 hour up to slightly more than 2 hours, depending on the time of day: in the hot seasons the phase-lag observed at the first minimum is the shortest whereas the phase-lags of the maxima and of the other minimum are larger, with the only exception of the second maximum of season SS2. These results suggest that further investigations about the phase-lag between atmospheric pressure and air temperature in caves should also consider the time of day at which the phase-lag is measured. The difficulties in accurately defining the exact time at which the minima and maxima occur increase the complexity of a thorough quantitative analysis of the phenomenon.

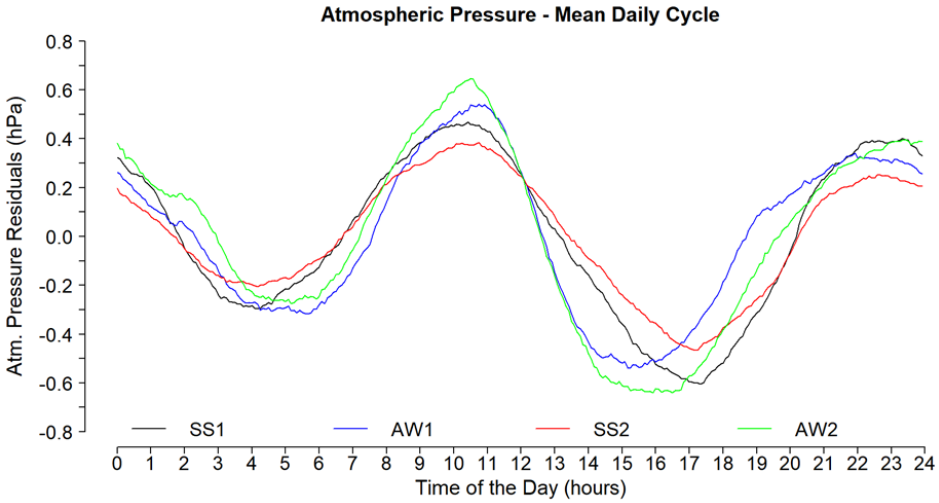

Figure 14: Mean daily cycle of atmospheric pressure in Doria cave.

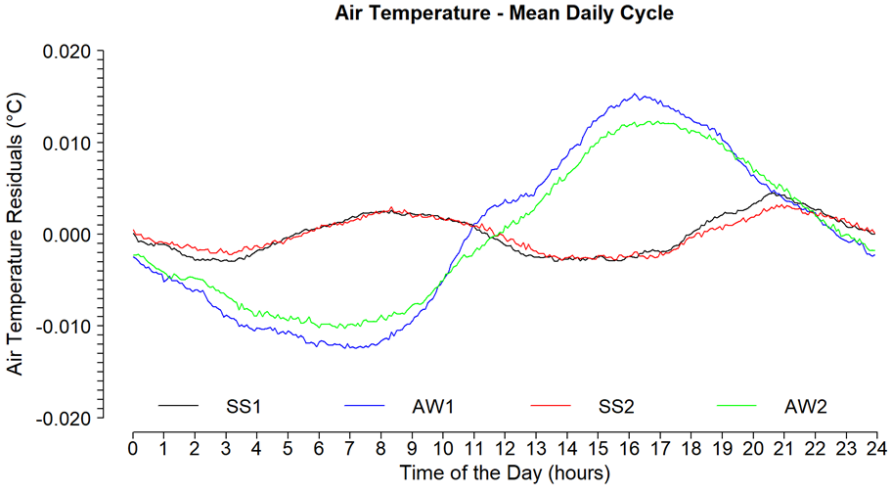

Figure 15: Mean daily cycle of air temperature in Doria cave.

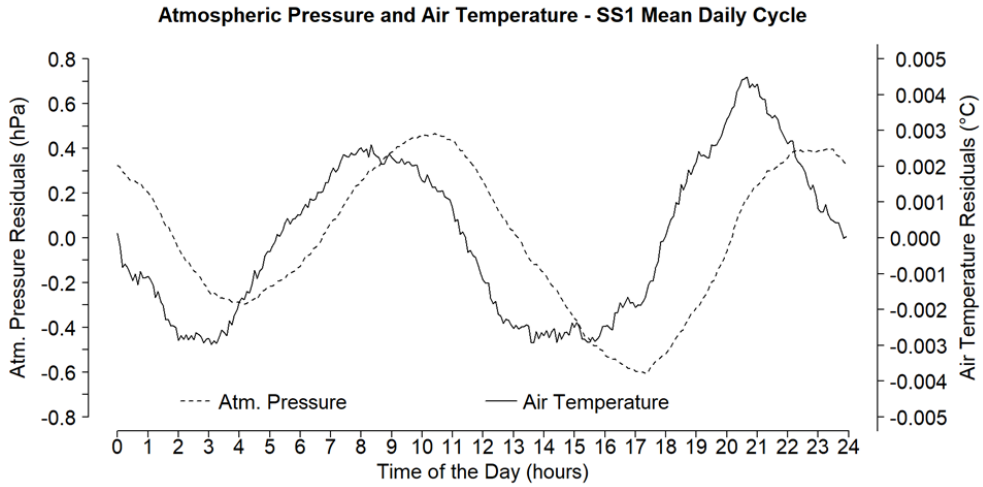

Figure 16: Phase-lag between the atmospheric pressure and the air temperature in Doria cave during season SS1.

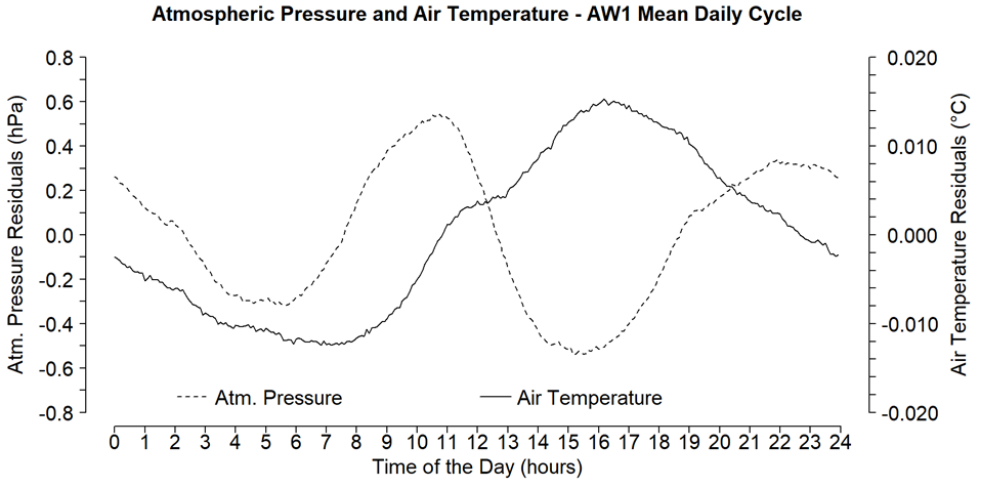

Figure 17: Phase-lag between the atmospheric pressure and the air temperature of Doria cave for season AW1.

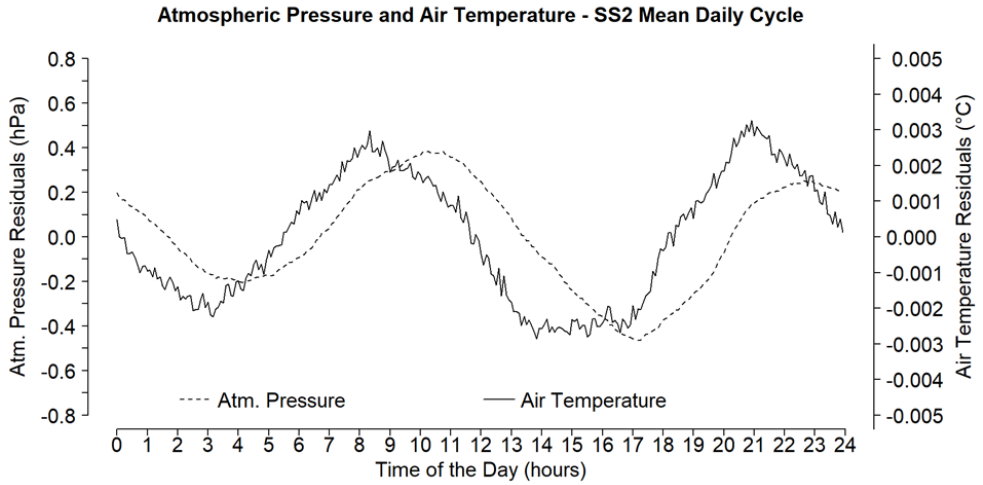

Figure 18: Phase-lag between the atmospheric pressure and the air temperature of Doria cave for season SS2.

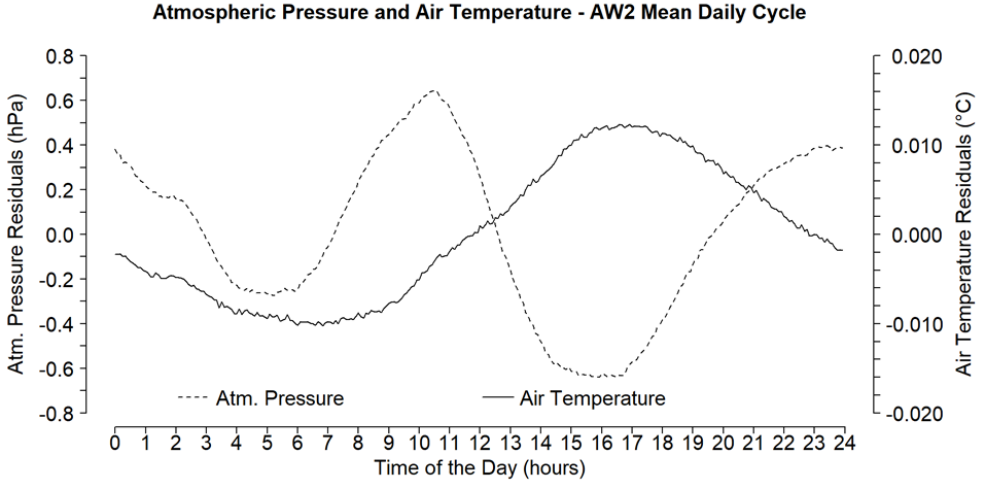

Figure 19: Phase-lag between the atmospheric pressure and the air temperature of Doria cave for season AW2.

CONCLUSION

In this paper, we analysed the seasonal characteristics of the atmospheric thermal tides, as observed both in the atmospheric pressure and in the air temperature signals of Costantino Doria cave. To the best of our knowledge, this is the first time that the seasonal effects of the atmospheric thermal tides on the air temperature of either a natural or an artificial cavity are investigated. Taking into account the presence of periodical constituents in both atmospheric pressure and air temperature of the cave, as well as considering the cave temperature oscillations about the trend, we identified two distinct seasons in Doria cave: a hot season, from mid-spring to mid-autumn, when the semidiurnal constituent is dominant in the air temperature and the thermal variations on a daily scale are minor (about one hundredth of degree), and a cold season, during which the 24-hours constituent of the air temperature of the cave is one order of magnitude higher than the 12-hours constituent and the oscillations of the cave temperature on a daily scale are much larger (about one tenth of degree). The two seasons correspond to two strongly different thermal regimes: on one hand, cold air filling and basically sealing the cave, and getting slowly heated by the rock walls in the hot season; on the other hand, external, denser cold air sinking into the cave from outside, causing a dramatic increase in the cave temperature variability in the cold season.

The analysis of the phase-lag between the atmospheric pressure and the air temperature signals of the cave showed that in both hot seasons – but not in the cold seasons – a phase-lag between the air temperature and the atmospheric pressure signal was present, with the air temperature peaking ahead of the atmospheric pressure of about 1-2 hours, according to the time of day. These results are in slight disagreement with what Chen et al. (2003), Wu et al. (2003), and Bussani (2005; 2007) had previously found. Therefore, we suggest that any further research about the effects of the atmospheric thermal tides on the air temperature signal of either natural or artificial cavities should take into account the seasonal characteristics of the meteorological parameters of the investigated environment.

ACKNOWLEDGMENTS

This work is dedicated to the memory of Mario Bussani, who in 2001 pushed us to resume the research activities of the meteorological characteristics of Costantino Doria cave. The authors wish to thank Aldo Fedel and Diadora Bussani for the help with the data collection in Doria cave, the Società Alpina delle Giulie - Commissione Grotte "Eugenio Boegan" and Renato R. Colucci for managing the Borgo Grotta Gigante weather station facilities, the Regional Weather Observatory of Friuli Venezia Giulia (Osmer - Osservatorio Meteorologico Regionale FVG) for making available the meteorological data of Borgo Grotta Gigante weather station, the Società Alpina delle Giulie - Commissione Grotte "Eugenio Boegan" for letting us access the Costantino Doria cave to perform this research, Igor Ardetti for valuable comments about some aspects of the research, Veronica Bonelli for reviewing the English language.

REFERENCES

BUSSANI A., 2005: "*Influenza delle maree atmosferiche sulle misure di temperatura registrate nella grotta 'C. Doria' (N. 3875 V.G.)",* Atti e Memorie, 40: 125-131

BUSSANI A., 2007: "*Atmospheric tide effects in a Trieste Karst cave: preliminary results",* Atti e Memorie, 41: 17-24

CHEN F., WU S., FAN S., LUO J, 2003: *"Determining the phases of the semidiurnal temperature and pressure oscillations by the cross-correlation equilibrium method",* Measurement Science and Technology, 14 (5): 619-624

CHOPPY J., 1980: "*Interpretation des mesures climatiques dans la grotte Costantino Doria (N. 3875 VG), publiées par S. Polli",* Atti e Memorie, 20: 21-53

EATON J. W., BATEMAN D., HAUBERG S., WEHBRING R., 2022: "*GNU Octave version 7.1.0 manual: a high-level interactive language for numerical computations",* https://www.gnu.org/software/octave/doc/v7.1.0/

FORTI F., TOMMASINI T., 1957: *"Strumentazione della grotta sperimentale 'Costantino Doria'"*, Alpi Giulie, 54 (1): 31-33

POLLI S., 1969: "*Meteorologia ipogea nella grotta 'C. Doria' del Carso di Trieste. Quinquennio 1963-67".* Atti e Memorie, 9: 87-98

R CORE TEAM, 2022: *"R: A language and environment for statistical computing"*, R Foundation for Statistical Computing, Vienna, Austria, URL https://www.R-project.org/

WU S., CHEN F., FAN S., LUO J., 2003: "*Phase leading of temperature variations in a cavity caused by heat conduction between air and rock",* Chinese Physics Letters, 12: 2192-2194

This paper was published online in November 2022 - www.boegan.it

Testo pubblicato in rete nel novembre 2022 su www.boegan.it